ГЛАСНИК Српског географског друштва 103(2) 145-160
BULLETIN OF THE SERBIAN GEOGRAPHICAL SOCIETY 2023

Original scientific paper
UDC 556.166(65)
https://doi.org/10.2298/GSGD2302145L

Received: May 25, 2023
Corrected: June 20, 2023
Accepted: June 23, 2023

Lamia Leulmi[1*], Youcef Lazri[**], Brahim Abdelkebir[***], Sofiane Bensehla[**]

** University of 8 Mai 1945, Department of Architecture, Hydraulic and civil engineering Laboratory (L.H.G.C), Guelma, Algeria*
*** University of 8 Mai 1945, Department of Architecture, Guelma, Algeria*
**** Laboratoire de génie civil et d'hydraulique, Université 8 mai 1945 - Guelma, Guelma, Algeria*

ASSESSMENT OF THE EFFECT OF LAND USE AND LAND COVER (LULC) CHANGE ON DEPTH RUNOFF: CASE STUDY OF SKIKDA FLOODS EVENT

Abstract: Land use and land cover changes in coastal cities can influence drainage systems in ways that affect surface overflows and the infiltration potential of a land surface, making flooding one of the drivers. This research aims to demonstrate the spatiotemporal dynamics of LULC and their combined impact on rainfall and flood height in Skikda, Algeria. The research uses remote sensing (RS) and geographic information systems (GIS) to determine the type and location of LULC changes in Skikda. The supervised classification methodology used the maximum likelihood technique (MCL). Changes were identified in five categories: built-up areas, green spaces, bodies of water, agriculture, and vacant land. In Q-GIS 3.28.2, Landsat 4-5 (TM) data from 1984 and 2004 and Landsat 8-9 (OLI)/TIRS data from 2019 were used based on the United States Geological Survey (USGS). The results show that the impervious built-up area has changed significantly (44.01%) due to massive urbanization and rapid industrialization, which would affect heavy rainfall activity and increase flood height due to the intense imperviousness of the affected soil (from 27% to 44%). The precipitation and flood height were examined and compared with observations to investigate the impact of the LULC model modification during the flood. The comparison of three flood events (1984, 2004, and 2019) revealed that the change in the LULC model is the main factor increasing flood risk in the study area. This study demonstrates the importance of considering temporal changes in land use, land cover, rainfall, and flood height when mapping floods in urban cities.

Key words: LULC change, flood risk, extreme rainfall, flood height, Skikda

[1] leulmi.lamia@univ-guelma.dz (corresponding author)

Introduction

The urban environment frequently fails to provide a high quality of life and causes conflicts with the natural environment (Miguez et al., 2019; Romero-Lankao et al., 2016). Thus, urban areas are more vulnerable to flooding (Salazar-Briones et al., 2020). Examples include Wuhan (Wang et al., 2022) and Chengdu (Li et al., 2023) in China; Paris (Toubin, 2015); Mindanao in the Philippines; Sylhet in Bangladesh; and Humacao on the island of Puerto Rico (Germanwatch et Munich RE NatCatservice, 2021). The Mediterranean rim's rainfall hazards (Deshons, 2002) are exacerbated by meteorological, hydrological, geographical, and geological factors. Furthermore, anthropogenic activities such as global warming, intensive exploitation of natural resources due to population growth, soil sealing, construction on land bordering watercourses, non-compliance with precautionary principles of river sedimentation, and inappropriate land use have increased the frequency and magnitude of floods over time (Samarasinghe et al., 2022; Yousuf & Romshoo 2022).

Floods are considered the most unpredictable geographical phenomenon that Algeria has experienced in recent decades due to the extent of material and immaterial damage caused, endangering human life (Mokhtari et al., 2023). Floods caused by heavy rains appear to be common in large catchment areas of the country, as evidenced by floods in December 1984 over eastern Algeria, Bab el Oued in 2001, and Ghardaa in 2008 (NOURI et al., 2016). Since the beginning of the land use and land coverage project (Debnath et al., 2023; Feizizadeh et al., 2023; Liping et al., 2018; Lucchetta et al., 2023), urbanization has been considered an important factor in changing land use and land coverage LULC (Abdelkebir et al., 2021). This results in the highest drainage value in urban areas, resulting in regular flood collection areas (Fernández & Lutz, 2010). The LULC model can analyse past changes and effectively simulate future changes, reducing LULC's complexity. The combination of remote sensing technology (RS) and geographic information system (GIS) has a strong approach to quantifying space and temporal phenomena with a broad range of perspectives and high accuracy (Kantakumar & Neelamsetti, 2015; Kordelas et al., 2018; Lo & Choi, 2004; Notti et al., 2018).

The study's overarching goal is to investigate the impact of land use and land cover change (LULC) on extreme precipitation and flood height recorded in 1984, 2004, and 2019 in a coastal area of Skikda in north-eastern Algeria using remote sensing and GIS techniques to better understand the mechanisms of urban flooding. The specific objectives of this study are as follows: (1) to quantitatively analyse and map the changes in LULC in Skikda using satellite images from 1984, 2004, and 2019; (2) to identify historical floods using time series of hydrological factors; and (3) to statistically study the impacts of LULC change on the variation of the selected hydrological factors: imperviousness, rainfall, and flood height.

Materials and methods

Study area

The study area (Figure 1) is a coastal commune and one of the country's primary industrial towns, serving an important regional role. It is 345 km east of Algiers (capital) in northeast Algeria, north of the wilaya of Skikda. The city has an area of 55.44 km² and a population of approximately 202,567 (ONS Skikda, 2023), accounting for more than 19% of the

wilaya's total population. Its latitude and longitude coordinates are 36° 52' 00" N and 6° 54' 00" E. The climate in this region is subhumid, rainy, and humid Mediterranean (hot and dry summer, heavy winter rainfall). Because of its relief, it is one of Algeria's most watered regions; the precipitation is 700 mm to 1200 mm of water per year, sometimes reaching 1800 mm yearly. The city is drained by two permanent rivers, Saf-Saf and Zramena, which originate a few kilometers from the sea and flow through a low, flat urban agglomeration (the industrial area, the Skikda agglomeration) surrounded by high mountains (Figure 2). The study area's unique geomorphic configuration, the city's constant rate of urbanization, and the area's variable hydrological conditions make it extremely vulnerable to violent and widespread fringed floods. During the flood season, the Saf-Saf and Zeramna rivers submerge the bordering areas, causing severe damage, reflecting the area's high vulnerability to floods.

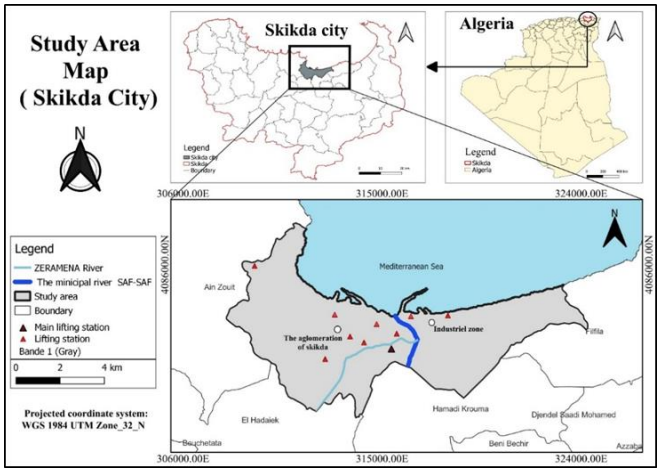

Fig. 1. Map of the study area, Skikda, Algeria

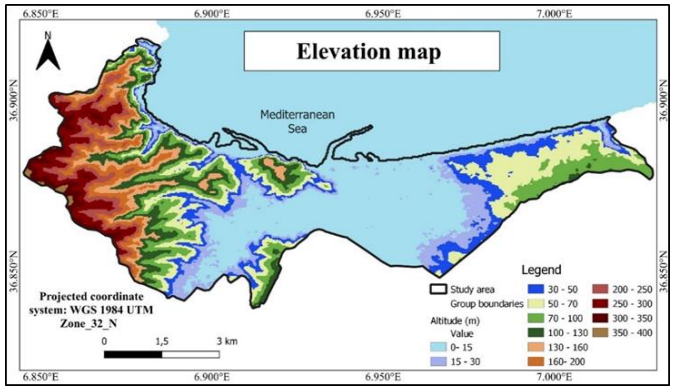

Fig. 2. Elevation map of the study area

Methodology

The vulnerability and harm indicators of urban systems cause flood risk. The LULC map is one of the most important spatial indicators of the severity of the quantitative flood (Waghwala & Agnihotri, 2019). The term “land use” is commonly used to refer to 'anthro-

pogenic land use' and the development of the land's surface. It is useful for navigation, infiltration rate, groundwater load, soil erosion, and hydrological modelling (Abdelkebir et al., 2021; Sugianto et al., 2022). Remote control and GIS-based change detection methods are widely used due to their low cost and high temporal resolution. The primary goal of this research is to examine the impact of LULC changes on extreme hydrology and flood risk using space LULC analysis in a GIS environment.

In this study, the quantitative supervised classification method was used to support LULC discovered from satellite images (Beroho et al., 2023; Campbell & Wynne, 2011; Seyam et al., 2023; Vivekananda et al., 2021). The UTM WGS 1984 Zone_32_N projection system was used for image processing. This method entails an image analyst supervising pixels via a specific algorithm, which provides a numerical explanation of the various types of land cover in the scene. The training locations are a sample of the identified cover type. The training sites are then used to compile a key that can explain the numerical value of various land covers expressed by spectral attributes for a specific type of interest.

The MLC maximum likelihood algorithm was used for medium-resolution satellite image data to determine land use and cover categorization (Do et al., 2022). The probability function underpins the algorithm, which assumes that the training data for each class in each band is normally distributed. A pixel's likelihood of belonging to each of a predefined set of classes is calculated, and the pixel is then assigned to the class with the highest probability (Basukala et al., 2017; Dalponte et al., 2008). The software Q-GIS 3.28.2 (Quantum-GIS) was used for analysis, classification of satellite images, and other area calculations. It is an open-source, cross-platform geographic information system (GIS) software created in 2002 to collect, process, analyze, manage, and present various geographic and spatial data types. To aid understanding of the process, the workflow for this study is represented on a methodological flowchart (Figure 3). Following that, the flowchart descriptions are given in the following sections.

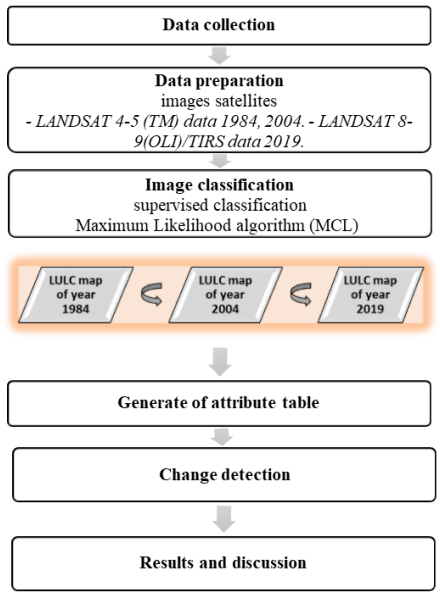

Fig. 3. Land use methodology flowchart (LULC) applied in this study

Data collection

A significant component of this study is the collection of primary and secondary data. The years 1984, 2004, and 2019 were chosen as reference years to discriminate and detect changes based on the key stages of the most severe floods recorded by ANRH (Skikda) and Skikda's infrastructure planning, which began rapidly after the territorial division in 1971. The collected data were classified as satellite and other auxiliary data (Table 1). Table 2 shows the basic characteristics of the satellite data used in the survey.

Tab. 1. Datasets and their source

Data used	Resolution scale	Format	Acquisition date	Source
Rainfall data and water level	62 years (1957-2019)	Text - District	2023	Algerian National Hydraulic Resources Agency - *ANRH*
SRTM	30 m	Satellite image	2023	https://earthexplorer.usgs.gov/.
2 LANDSAT : ▪ Landsat-5TM. ▪ LANDSAT 8-9(OLI).	30 m	Satellite image	2023	https://earthexplorer.usgs.gov/
Administrative divisions	/	Shape file-Polygon	2023	Algerian National Hydraulic Resources Agency - *ANRH*

Tab. 2. Main characteristics of the Landsat satellite data used in this study

Scene ID	Raw/ Path	Source	Year	Satellite &Sensor	Acquisition date	Resolution
LT05_L1TP_193034_19841203_20200918_02_T1	137/43	USGS	1984	Landsat-5TM	1984-12-03	30 m
LT05_L1TP_193034_20040223_20200903_02_T1	137/43	USGS	2004	Landsat-5TM	2004-02-23	30 m
LC08_L1TP_193035_20190216_20200829_02_T1	137/43	USGS	2019	Landsat 8 OLI/TIRS	2019-02-16	30m

Data preparation

Landsat 5 Thematic Mapper (MT) images from 1984 and 2004 and the Landsat 8 Operational Land Imager (OLI) image from 2019 were used to classify and detect LULC changes in Skikda. Landsat 5 and 8 images in Skikda have been geographically adjusted to UTM WGS 1984 Zone 32_N coordinates to synchronize the coordinates and facilitate the calculation of fluctuations. Satellite data covering the study site was obtained from the official United States Geological Survey (USGS) website: (https://www.usgs.gov/.), which can be downloaded for free anywhere in the world and contains a wealth of information for identifying and monitoring changes in manufactured and physical environments (El Bastawesy, 2015). The data was downloaded in GeoTIFF format. The corrected base map of the study area was obtained from the Skikda Centre of Geographical Data.

Each Landsat ETM, Landsat 5, and Landsat 8 data set comprises separate, independent banded images stacked and combined to form a multi-band image. The map classes for 1984 and 2004 were determined using the Band Composition for Landsat 5 for 2019 and the Band Composition for Landsat 8. The spatial resolution of these images is 30 m per pixel. Landsat images were chosen for the study area based on cloud-free, clear, and

available years. We used DEM and the well-known Shuttle Radar Topography Mission (SRTM) data from https://earthexplorer.usgs.gov/ with a resolution of 30 m. QGIS 3.28.2 software was used to process the satellite data. We chose the period of the deviating floods in recent years for the rainfall and flood height data (Table 1). They were used as forcing data for flood events.

LULC extraction

A classification approach tailored to the search area is required first and foremost to categorize satellite images based on similar or identical spectral reflectance properties. As a result, several LULC shapes are classified in this study using a supervised classification approach. For Landsat imagery, the supervised classification approach was used in QGIS version 3.28.2 with a maximum likelihood algorithm (MCL) to classify geo-referenced digital data from satellite imagery for 35 different years, from 1984 to 2019, at three different time scales: 1984, 2004 and 2019. The areas were classified based on their land use. Land cover information was collected randomly, and purposive sampling was used to identify locations for infiltration data collection. The classified raster images were converted into vector layers before classification. Each class was created using texture, tone, and colour. In the image classification, these classes were assigned to the pixels. Five LULC classes were identified within the study area: i) urban; ii) green space; iii) water bodies; iv) agriculture; and v) bare land. Table 3 describes the specifics of each land use/land cover type. For the calculation, the total study area for both years was 55.44 km². The percentage of various LULC categories and the total area of these LULC classes were expressed. Following the formula below, the statistics were compiled and used to estimate the imperviousness (1), which represents the ratio of impervious area to total area considered:

$$\text{Impermeability coefficient} = \sum (\text{impermeable surface})/(\text{total surface}) \quad (1)$$

Tab. 3. Description of the classes delineated based on supervised classification of land use types in the study area

Type of land cover	**Description**
Urban building	Concrete buildings, commercial/residential structures, industrial areas, paved surfaces and roads, mixed urban, educational institutions, transportation, open-roof concrete structures, other manufactured structures, and solid waste dumps are all included in this category.
Green space	Plantations, plantations, forest production areas, grasslands, and herbs
Waterbody	It encompasses all water-covered areas, including seasonal/permanent rivers, streams, lakes, gravels, open waters, creeks, dams, canals, and reservoirs.
Agriculture	Include all cultivated land with a high population density and other agricultural land.
Bar ground	Areas with sparse vegetation are expected to change or be converted to other users. This category includes land without crops, barren rocks, and sandy sections along river beaches.

LULC change detection analysis

The maximum likelihood supervised classification method was used in this study to detect and evaluate land cover changes. The LULC area was calculated for each land cover type, and the results were compared by class. Cross-tabulations were used to compare classified images from three other datasets to determine changes' qualitative and quantitative as-

pects in 1984, 2004, and 2019. The magnitude of change in the area and the percentage of the changing trend were examined.

Result and discussion

LULC model of Skikda in 1984, 2004 and 2019

Figure 5 depicts a schematic representation of the spatial distribution pattern of land cover and land use obtained after surface classification in 1984, 2004, and 2019. The distribution of the calculated area of land types in square kilometres and percentages for 1984, 2004, and 2019 is shown in Tables 4 and 5 and Figure 4. According to the maps, the built environment is the largest group, nearly tripling from 1984 to 2019 (15.29 km², 22.07 km², and 24.40 km², respectively). Green spaces occupy the second-largest group of land areas, with 16.01 km², 16.20 km², and 15.35 km², respectively, according to data from 1984, 2004, and 2019. Meanwhile, the water body, which was only 1.10 km² in 1984, has grown to 2.08 km² in 2004 and 3.07 km² in 2019.

However, the area of agricultural land in the study area has decreased sharply, from 15.28 km² in 1984 to 7.93 km² in 2004 and then to 5.36 km² in 2019, indicating a significant loss of agricultural land in the study area for residential and industrial facilities due to population growth and industrialization policy. This has also occurred in the bare land cover, which has decreased by 0.5 km² throughout the study. Between 1984 and 2019, LULC patterns shifted dramatically. The printability coefficient rose by 0.27, 0.39, and 0.44 in 1984, 2004 and 2019. As more water remains on the surface, this increasing imperviousness raises the risk of flooding in the study area. However, the floodplain has experienced significantly higher flow rates; this overflow has been difficult to evacuate, resulting in significant flooding.

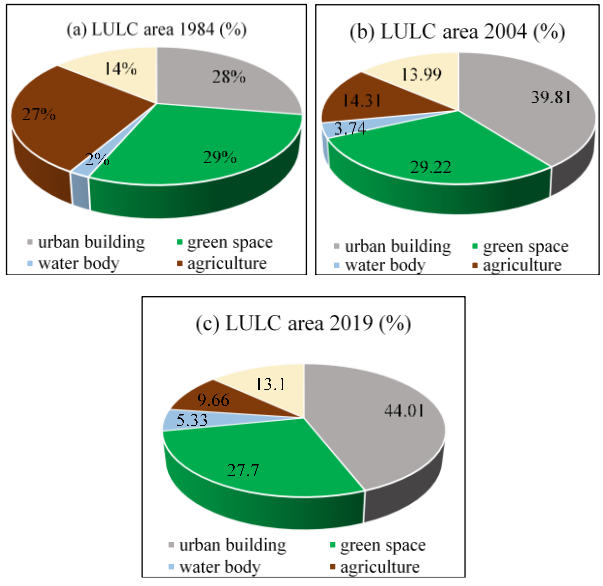

Fig. 4. Pie chart showing the percentage distribution of study area land use in 1984, 2004, and 2019, with (a), (b), and (c), respectively

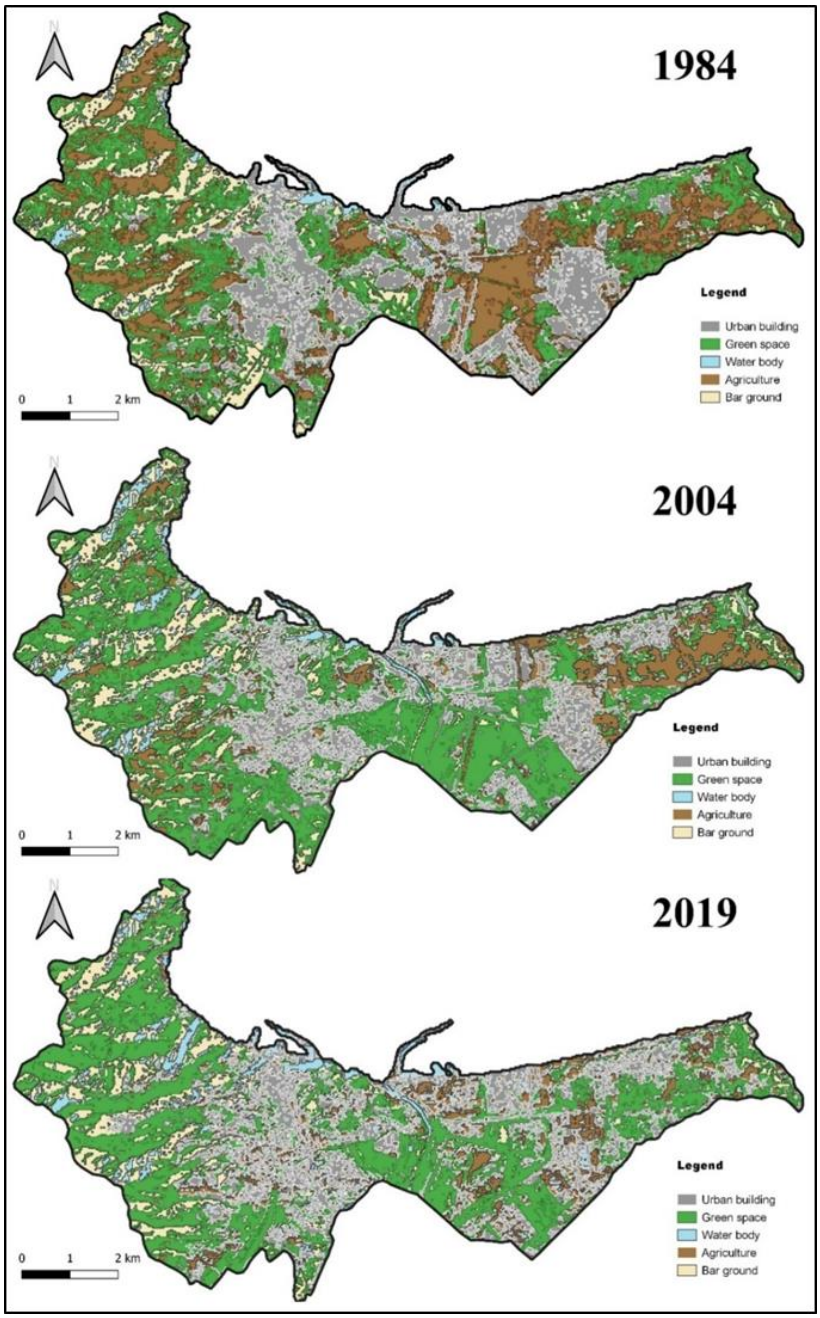

Fig. 5. Skikda commune land use scenarios by LULC classification in 1984, 2004, and 2019, respectively

Tab. 4. Area and quantity of land use in Skikda commune in 1984, 2004, and 2019

Date	Land use areas					
	1984		2004		2019	
Class	Sq. km²	%	Sq. km²	%	Sq. km²	%
Urban building	15.29	27.59	22.07	39.81	24.40	44.01
Green space	16.01	28.88	16.20	29.22	15.35	27.70
Waterbody	1.10	1.99	2.08	3.74	3.04	5.53
Agriculture	15.28	27.55	7.93	14.31	5.36	9.66
Bar ground	7.76	13.99	7.16	12.92	7.26	13.10
Total	55.44	100.00	55.44	100.00	55.44	100.00
Coefficient of impermeability	0.27	27.00	0.39	39.00	0.44	44.00

Tab. 5. Results of the extent of land use change in the commune of Skikda in 1984, 2004 and 2019

Date	Magnitude of land use change					
	1984- 2004		2004- 2019		1984-2019	
Class	Sq. km²	%	Sq. km²	%	Sq. km²	%
Urban building	+6.78	+12.22	+2.33	+4.20	+9.11	+16.42
Green space	+0.19	+0.34	-0.85	-1.52	-0.66	-1.18
Waterbody	+0.98	+1.75	+0.99	+1.79	+1.97	+3.54
Agriculture	-7.35	-13.24	-2.57	-4.65	-9.92	-17.89
Bar ground	-0.60	-1.07	+0.10	+0.18	-0.50	-0.89
Total	0	0	0	0	0	0
Coefficient of impermeability	+0.12	12	+0.5	5	+0.17	17

Detection of LULC changes from 1984, 2004 and 2019

The data in Table 4 and Figure 5 show that the Skikda land use and cover model has changed positively and negatively. The difference in area between 1984 and 2019 for each class was used to calculate the LULC change in land use, as shown in Figure 6. The study area's land use statistics show changes in all land uses. Agriculture and bare land have decreased by 9.90 km², or about 18%, and 0.5 km², respectively, during the study period. Nonetheless, between 1984 and 2019, green space decreased by about 2%. The water area has increased by 1.97 km² or 0.06 km² per year. After 1984, the built-up area nearly tripled, with an average annual increase of 0.26 km² and an average annual growth rate of land use of 0.3 km². If the growth rate in residential land use in the Skikda area is assumed to be constant at 0.3 km² per year, this area will occupy 32.5 km², or approximately 58.62% of the city's total area, in 2050.

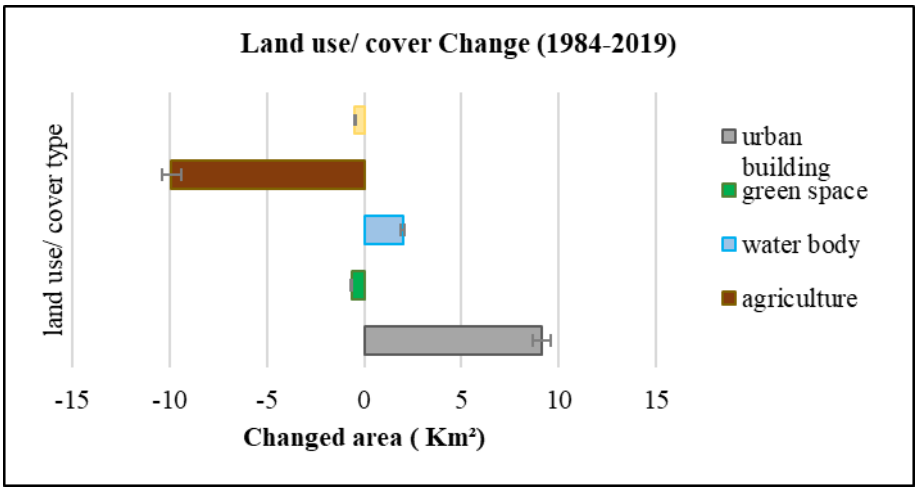

Fig. 6. Diagram of land use/land cover change in the study area in 1984, 2004, and 2019

Determination of flood history

Disastrous floods have plagued Skikda since ancient times. Figure 7 depicts the flood history of the study area, highlighting the severe floods recorded in the area. The most destructive events occurred on November 21-23, 1957, 11-17, 1958, 1973, February 4, 1984, December 30, 1984-1985 (5 days were single), December 2002, 13-14, November 2004, 2-3, February 2011, and January 9, 2019 (civil protection - Skikda). In particular, floods of 84 and 85 were the largest ever recorded in northeastern Algeria based on annual, monthly, and daily rainfall records. The basin received a cumulative rainfall of 401.3 mm, resulting in an exceptional peak flow of 404 m^3/s to 741.3 m^3/s. The consequences were severe: massive loss of life (11 people died) and economic losses, including agricultural losses (450 ha of fodder, 300 ha of citrus fruits, and 850 ha of cereals), destruction of buildings and infrastructures (174 houses demolished, and 500 families affected), flooding of the petrochemical industrial zone, and the five-day isolation of Skikda (National Water Resources Agency, ANRH).

The flood height and rainfall data were obtained as textual data from the Khemakhem hydrometric station. Between 1957 and 2019, an irregular annual rainfall pattern and its unfavourable evolution were observed. Overall, rainfall increased from 172.5mm to 745.1mm in the study area between 1957 and 1985, in response to the opening of the industrial zone following the country's industrialization policy in 1971, to the detriment of agriculture. The city of Skikda then experienced a significant decrease in rainfall when compared to 1980 and 1990. The study area is frequently flooded during winter (November to February).

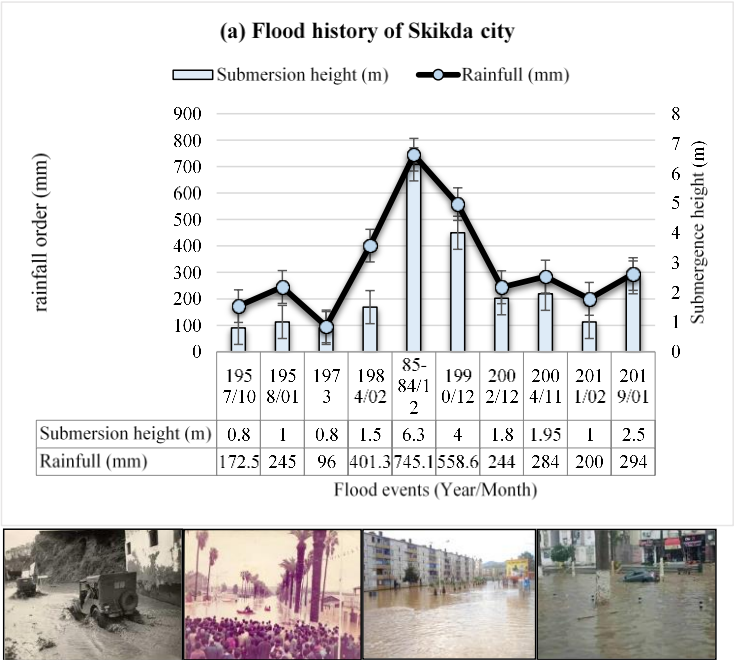

Fig. 7. (a) historical series of the most severe floods related to the orders of rainfall and water height recorded in the Khemakhem hydrometric station from 1957 to 2019; (b-e) images of urban floods in the Skikda commune. According to ANRH Skikda, the red boxes on the images may reflect the severity of the flooding (Authors, 2023)

Analysis of the interaction between LULC changes and hydrological factors (rainfall order and flood height)

When investigating the change in LULC of the study area and its direct influence on the flood peak, a complex relationship between the two factors began to emerge, allowing the main goal of this research to be met. Changes in LULC, particularly an increase in the impervious built environment, cause hydrological changes (temporal evolution of precipitation and flood height) in catchment areas and, in extreme cases, flooding if discharge exceeds total river flow. The interaction between land use, land cover, and flood height was studied using qualitative parameters from 1984 to 2019 (Figure 8). We discovered that for the 1984 LULC scenario, the imperviousness coefficient was 0.27 (the impervious area was 27.59%, green areas were 28.88%, and agricultural land was 27.55%); the water height was 6.30m NGA in response to the heavy rainfall event (190.5 mm - 745.1 m^3/s); occurring on December 30, 1984/85, for five days. While the rainfall was reduced to 125.7mm in the LULC scenario 2004, the analysis revealed that the flood height of 1.0 m was reduced due to a 12% increase in imperviousness, which reduced the infiltration capacity. For the 2019 LULC scenario, however, the water height was increased to 2.00 m in response to a 295 mm increase in rainfall and a 5% increase in imperviousness, reducing water infiltration from extreme rainfall. As a result, the overflow of Wadi Zeramna and Saf-Saf toward the adjacent lands has increased.

Over the last 30 years, uncontrolled urbanization and agricultural land consumption have occurred on floodplains throughout the study area, resulting in the siltation of wa-

tercourses. The study area's LULC conditions change with time and nature. Between 1984 and 2019, this variation occurred due to the transition from one LULC class to another. The conversion of agricultural land from temporary flood retention areas to built-up areas and rangeland has been reported as the most notable land cover change in Skikda since the 1980s, driven by population growth and the resulting need for housing and other necessary infrastructure, industrialization, economic expansion, and uncontrolled construction in the Oueds (Zeramena and Saf-saf). This has resulted in an increase in impervious surfaces, which prevents infiltration and reduces the environment's capacity to absorb excess stormwater, resulting in increased stormwater runoff and surface flow in the Zeramena sub-catchment. It should be noted that the rainfall is even slightly above average, causing flooding in the category of constructions, roads, railways, and other concreted spaces in the study area due to low imperviousness or storage capacity; thus, changes in LULC had a significant influence on soil infiltration.

As a result, a significant increase in flood volumes is expected, with flood waters causing more damage, particularly in these converted areas. The results show that variations in rainfall and flood height caused by LULC changes significantly impacted flood output in a semi-arid area (Skikda) between 1984 and 2019. These findings are consistent with those of (Abuhay et al., 2023; Apollonio et al., 2016; Darabi et al., 2019; Li et al., 2023; Olang & Fürst, 2011; Saghafian et al., 2008; Waghwala & Agnihotri, 2019) who worked on different watersheds and reached similar conclusions. The study focuses on the hydrological consequences of large land cover changes, where sudden flooding can be especially severe, particularly at small scales. As a result, to reduce the likelihood of flooding caused by ongoing climate and land use change, sustainable land use and watershed management strategies must be developed.

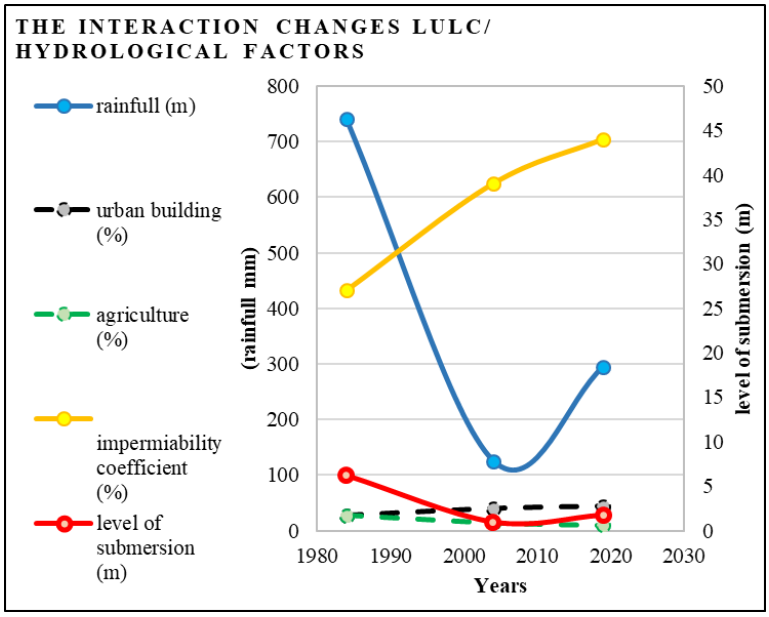

Fig. 8. Scenarios of contributing factors to flooding: LULC, printability coefficient, rainfall and flood height in the commune of Skikda; during the periods 1984, 2004 and 2019

Conclusion

This study was conducted in Skikda, Algeria, one of the emerging and rapidly growing regions for various industries, which has exacerbated the production of urban floods in recent years. Localized changes in LULC are the primary cause of frequent deviations from the global trend. A supervised quantitative classification method using a maximum likelihood MLC algorithm was used to examine the effect of LULC changes in an urban environment and their varying impact on hydrological processes and flood peaks while accounting for precipitation and flood height uncertainty. Landsat5 TM and Landsat 8 OLI image data were used in this study to create land use maps from 1984, 2004, and 2019. The study area's land use structure was simulated and predicted using a GIS environment.

The findings show significant changes in LULC, with impervious building land dominating and agriculture deteriorating rapidly. However, our findings confirmed that a significant change in LULC has been identified and that rapid urbanization and industrial activities have been the primary drivers of flood risk in the study area over the last few decades. As a result, it concludes that this information will be useful for policymakers and regional development planners to be aware of Skikda's rapid development and changes in land use patterns.

Conflicts of Interest: The authors declare no conflict of interest.

Publisher's Note: Serbian Geographical Society stays neutral with regard to jurisdictional claims in published maps and institutional affiliations.

References

Abdelkebir, B., Maoui, A., Mokhtari, E., Engel, B., Chen, J., & Aboelnour, M. (2021). Evaluating Low-Impact Development practice performance to reduce runoff volume in an urban watershed in Algeria. *Arabian Journal of Geosciences, 14*(9), 814. https://doi.org/10.1007/s12517-021-07178-0

Abuhay, W., Gashaw, T., & Tsegaye, L. (2023). Assessing impacts of land use/land cover changes on the hydrology of Upper Gilgel Abbay watershed using the SWAT model. *Journal of Agriculture and Food Research, 12*, Article 100535. https://doi.org/10.1016/j.jafr.2023.100535

Apollonio, C., Balacco, G., Novelli, A., Tarantino, E., & Piccinni, A. (2016). Land Use Change Impact on Flooding Areas: The Case Study of Cervaro Basin (Italy). *Sustainability, 8*(10), 996. https://doi.org/10.3390/su8100996

Basukala, A. K., Oldenburg, C., Schellberg, J., Sultanov, M., & Dubovyk, O. (2017). Towards improved land use mapping of irrigated croplands: Performance assessment of different image classification algorithms and approaches. *European Journal of Remote Sensing, 50*(1), 187-201. https://doi.org/10.1080/22797254.2017.1308235

Beroho, M., Briak, H., Cherif, E.K., Boulahfa, I., Ouallali, A., Mrabet, R., Kebede, F., Bernardino, A., & Aboumaria, K. (2023). Future Scenarios of Land Use/Land Cover (LULC) Based on a CA-Markov Simulation Model: Case of a Mediterranean Watershed in Morocco. *Remote Sensing, 15*, 1162. https://doi.org/10.3390/rs15041162

Campbell, J. B., & Wynne, R. H. (2011). *Introduction to Remote Sensing* (5th ed.). The Guilford Press.

Dalponte, M., Bruzzone, L., & Gianelle, D. (2008). Fusion of Hyperspectral and LIDAR Remote Sensing Data for Classification of Complex Forest Areas. *IEEE Transactions on Geoscience and Remote Sensing, 46*(5), 1416-1427. https://doi.org/10.1109/TGRS.2008.916480

Darabi, H., Choubin, B., Rahmati, O., Torabi Haghighi, A., Pradhan, B., & Kløve, B. (2019). Urban flood risk mapping using the GARP and QUEST models: A comparative study of machine learning techniques. *Journal of Hydrology, 569*, 142-154. https://doi.org/10.1016/j.jhydrol.2018.12.002

Debnath, J., Sahariah, D., Lahon, D., Nath, N., Chand, K., Meraj, G., Kumar, P., Kumar Singh, S., Kanga, S., & Farooq, M. (2023). Assessing the impacts of current and future changes of the planforms of river Brahmaputra on its land use-land cover. *Geoscience Frontiers, 14*(4), 101557. https://doi.org/10.1016/j.gsf.2023.101557

Deshons, P. (2002). Prévision et suivi des crues urbaines Expérience de la ville de Marseille. *La Houille Blanche, 88*(2), 56-59. https://doi.org/10.1051/lhb/2002022

Do, T. A. T., Do, A. N. T., & Tran, H. D. (2022). Quantifying the spatial pattern of urban expansion trends in the period 1987–2022 and identifying areas at risk of flooding due to the impact of urbanization in Lao Cai city. *Ecological Informatics, 72*, 101912. https://doi.org/10.1016/j.ecoinf.2022.101912

El Bastawesy, M. (2015). The geomorphological and hydrogeological evidences for a Holocene deluge in Arabia. *Arabian Journal of Geosciences, 8*(5), 2577-2586. https://doi.org/10.1007/s12517-014-1396-9

Feizizadeh, B., Omarzadeh, D., Kazemi Garajeh, M., Lakes, T., & Blaschke, T. (2023). Machine learning data-driven approaches for land use/cover mapping and trend analysis using Google Earth Engine. *Journal of Environmental Planning and Management, 66*(3), 665-697. https://doi.org/10.1080/09640568.2021.2001317

Fernández, D. S., & Lutz, M. A. (2010). Urban flood hazard zoning in Tucumán Province, Argentina, using GIS and multicriteria decision analysis. *Engineering Geology, 111*(1-4), 90-98. https://doi.org/10.1016/j.enggeo.2009.12.006

Kantakumar, L. N., & Neelamsetti, P. (2015). Multi-temporal land use classification using hybrid approach. *The Egyptian Journal of Remote Sensing and Space Science, 18*(2), 289-295. https://doi.org/10.1016/j.ejrs.2015.09.003

Kordelas, G., Manakos, I., Aragonés, D., Díaz-Delgado, R., & Bustamante, J. (2018). Fast and Automatic Data-Driven Thresholding for Inundation Mapping with Sentinel-2 Data. *Remote Sensing, 10(*6), 910. https://doi.org/10.3390/rs10060910

Li, Y., Osei, F. B., Hu, T., & Stein, A. (2023a). Urban flood susceptibility mapping based on social media data in Chengdu city, China. *Sustainable Cities and Society, 88*, 104307. https://doi.org/10.1016/j.scs.2022.104307

Liping, C., Yujun, S., & Saeed, S. (2018). Monitoring and predicting land use and land cover changes using remote sensing and GIS techniques—A case study of a hilly area, Jiangle, China. *PLOS ONE, 13*(7), e0200493. https://doi.org/10.1371/journal.pone.0200493

Lo, C. P., & Choi, J. (2004). A hybrid approach to urban land use/cover mapping using Landsat 7 Enhanced Thematic Mapper Plus (ETM+) images. *International Journal of Remote Sensing, 25*(14), 2687-2700. https://doi.org/10.1080/01431160310001618428

Lucchetta, B. C., Watanabe, F. S. Y., & do Carmo, N. M. R. B. (2023). A spatiotemporal classification approach to evaluate the impacts of land use and land cover changes before and after the Três Irmãos reservoir formation in the Tietê River, Brazil. *Modeling Earth Systems and Environment*. https://doi.org/10.1007/s40808-023-01757-8

Miguez, M. G., Veról, A. P., Battemarco, B. P., Yamamoto, L. M. T., de Brito, F. A., Fernandez, F. F., Merlo, M. L., & Queiroz Rego, A. (2019). A framework to support the urbanization process on lowland coastal areas: Exploring the case of Vargem Grande – Rio de Janeiro, Brazil. *Journal of Cleaner Production, 231*, 1281-1293. https://doi.org/10.1016/j.jclepro.2019.05.187

Mokhtari, E., Mezali, F., Abdelkebir, B., & Engel, B. (2023). Flood risk assessment using analytical hierarchy process: A case study from the Cheliff-Ghrib watershed, Algeria. *Journal of Water and Climate Change, 14*(3), 694-711. https://doi.org/10.2166/wcc.2023.316

Nouri, M., Ozer, A., & Ozer, P. (2016). Etude préliminaire sur le risque d'inondation en milieu urbain (Algérie) Preliminary study on the flood risk in urban areas (Algeria). *Geo-Eco-Trop, 40*(3), 201-208.

Notti, D., Giordan, D., Caló, F., Pepe, A., Zucca, F., & Galve, J. (2018). Potential and Limitations of Open Satellite Data for Flood Mapping. *Remote Sensing, 10*(11), 1673. https://doi.org/10.3390/rs10111673

Olang, L. O., & Fürst, J. (2011). Effects of land cover change on flood peak discharges and runoff volumes: Model estimates for the Nyando River Basin, Kenya. *Hydrological Processes, 25*(1), 80-89. https://doi.org/10.1002/hyp.7821

Romero-Lankao, P., Gnatz, D., Wilhelmi, O., & Hayden, M. (2016). Urban Sustainability and Resilience: From Theory to Practice. *Sustainability, 8*(12), 1224. https://doi.org/10.3390/su8121224

Saghafian, B., Farazjoo, H., Bozorgy, B., & Yazdandoost, F. (2008). Flood Intensification due to Changes in Land Use. *Water Resources Management, 22*(8), 1051-1067. https://doi.org/10.1007/s11269-007-9210-z

Salazar-Briones, C., Ruiz-Gibert, J. M., Lomelí-Banda, M. A., & Mungaray-Moctezuma, A. (2020). An Integrated Urban Flood Vulnerability Index for Sustainable Planning in Arid Zones of Developing Countries. *Water, 12*(2), 608. https://doi.org/10.3390/w12020608

Samarasinghe, J. T., Gunathilake, M. B., Makubura, R. K., Arachchi, S. M. A., & Rathnayake, U. (2022). Impact of Climate Change and Variability on Spatiotemporal Variation of Forest Cover; World Heritage Sinharaja Rainforest, Sri Lanka. *Forest and Society, 6*(1). https://doi.org/10.24259/fs.v6i1.18271

Seyam, M. M. H., Haque, M. R., & Rahman, M. M. (2023). Identifying the land use land cover (LULC) changes using remote sensing and GIS approach: A case study at Bhaluka in Mymensingh, Bangladesh. *Case Studies in Chemical and Environmental Engineering, 7*, 100293. https://doi.org/10.1016/j.cscee.2022.100293

Sugianto, S., Deli, A., Miswar, E., Rusdi, M., & Irham, M. (2022). The Effect of Land Use and Land Cover Changes on Flood Occurrence in Teunom Watershed, Aceh Jaya. *Land, 11*(8), 1271. https://doi.org/10.3390/land11081271

Toubin, M. (2015). III. Améliorer la résilience urbaine par un diagnostic collaboratif—L'exemple des services urbains parisiens face à l'inondation. https://www.persee.fr/doc/coloc_2111-8779_2015_num_35_1_2945

Vivekananda, G., Swathi, R., & Sujith, A. (2021). Multi-temporal image analysis for LULC classification and change detection. *European Journal of Remote Sensing, 54*(sup2), 189-199. https://doi.org/10.1080/22797254.2020.1771215

Waghwala, R. K., & Agnihotri, P. G. (2019). Flood risk assessment and resilience strategies for flood risk management: A case study of Surat City. *International Journal of Disaster Risk Reduction, 40*, 101155. https://doi.org/10.1016/j.ijdrr.2019.101155

Wang, X., Xia, J., Zhou, M., Deng, S., & Li, Q. (2022). Assessment of the joint impact of rainfall and river water level on urban flooding in Wuhan City, China. *Journal of Hydrology, 613*, 128419. https://doi.org/10.1016/j.jhydrol.2022.128419

Yousuf, A., & Romshoo, S. A. (2022). Impact of Land System Changes and Extreme Precipitation on Peak Flood Discharge and Sediment Yield in the Upper Jhelum Basin, Kashmir Himalaya. *Sustainability, 14*(20), 13602. https://doi.org/10.3390/su142013602